Available online at www.sciencedirect.com
SCIENCE DIRECT
Journal of Sound and Vibration 293 (2006) 510–521
JOURNAL OF SOUND AND VIBRATION
www.elsevier.com/locate/jsvi

Multi-disciplinary optimization of railway wheels

J.C.O. Nielsen[a,b,*], C.R. Fredö[b]

[a]CHARMEC/Department of Applied Mechanics, Chalmers University of Technology, SE-412 96 Gothenburg, Sweden
[b]Ingemansson Technology AB, Kämpegatan 7, SE-401 24 Gothenburg, Sweden

Accepted 26 August 2005
Available online 15 February 2006

Abstract

A numerical procedure for multi-disciplinary optimization of railway wheels, based on Design of Experiments (DOE) methodology and automated design, is presented. The target is a wheel design that meets the requirements for fatigue strength, while minimizing the unsprung mass and rolling noise. A 3-level full factorial (3LFF) DOE is used to collect data points required to set up Response Surface Models (RSM) relating design and response variables in the design space. Computationally efficient simulations are thereafter performed using the RSM to identify the solution that best fits the design target. A demonstration example, including four geometric design variables in a parametric finite element (FE) model, is presented. The design variables are wheel radius, web thickness, lateral offset between rim and hub, and radii at the transitions rim/web and hub/web, but more variables (including material properties) can be added if needed. To improve further the performance of the wheel design, a constrained layer damping (CLD) treatment is applied on the web. For a given load case, compared to a reference wheel design without CLD, a combination of wheel shape and damping optimization leads to the conclusion that a reduction in the wheel component of A-weighted rolling noise of 11 dB can be achieved if a simultaneous increase in wheel mass of 14 kg is accepted.

1. Introduction

The stresses induced in a railway wheel due to wheel–rail contact loads and/or thermal braking loads strongly depend on the geometrical configuration of the wheel web (disc), see Fermér [1]. A so-called "low-stress" freight car wheel is often characterized by a curved web and a lateral offset between hub and rim. This leads to lower residual stresses and deformations induced by the heating and cooling connected with tread braking. The wheel design must also meet the requirements for high cycle fatigue strength to avoid failures due to cracking. On the other hand, by straightening the shape of the web to obtain a more symmetrical cross-section, the coupling of vertical and lateral vibrations, as excited by wheel–rail contact loads, will be reduced. Raising the stiffness of the web by increasing its thickness can move some wheel resonance frequencies out of the range of rolling excitation [2]. In addition, a constrained layer damping (CLD) treatment applied on the web can be successful in reducing vibrations if the added damping exceeds the effective "rolling damping"

*Corresponding author. Ingemansson Technology AB, Klubbhusgatan 13, SE-553 03 Jönköping, Sweden. Tel.: +46 31 772 1500; fax: +46 31 772 3827.
E-mail address: jens.nielsen@me.chalmers.se (J.C.O. Nielsen).

0022-460X/$ - see front matter
doi:10.1016/j.jsv.2005.08.063

generated by the dynamic interaction of train and track [3,4]. Means of reducing vibrations will lead to a simultaneous reduction in rolling noise generated by the wheel. Further, minimizing the unsprung mass of the wheelset will reduce dynamic wheel–rail contact loads [5]. In summary, a compromise is necessary to reach a wheel design that meets all requirements. An example of this was presented by Daneryd et al. [6], where an attempt was made to design a freight car wheel with a perforated web in order to reduce rolling noise through acoustic short-circuiting while obeying operational requirements with respect to fatigue and thermally induced residual stresses and deformations.

Here, the target is a disc-braked wheel design for high-speed traffic that meets the requirements for high-cycle fatigue strength, while minimizing dynamic wheel–rail contact loads (due to a reduced unsprung mass) and rolling noise (due to an optimized web shape with CLD). This calls for a multi-disciplinary approach involving design variables such as wheel radius, web thickness, hub/rim lateral offset and thickness of the visco-elastic damping layer. The objective of the paper is to suggest and demonstrate an automated optimization procedure that is computationally efficient in such wheel design. A flow diagram illustrating the procedure and the transfer of data between the adopted software is illustrated in Fig. 1. Commercial softwares

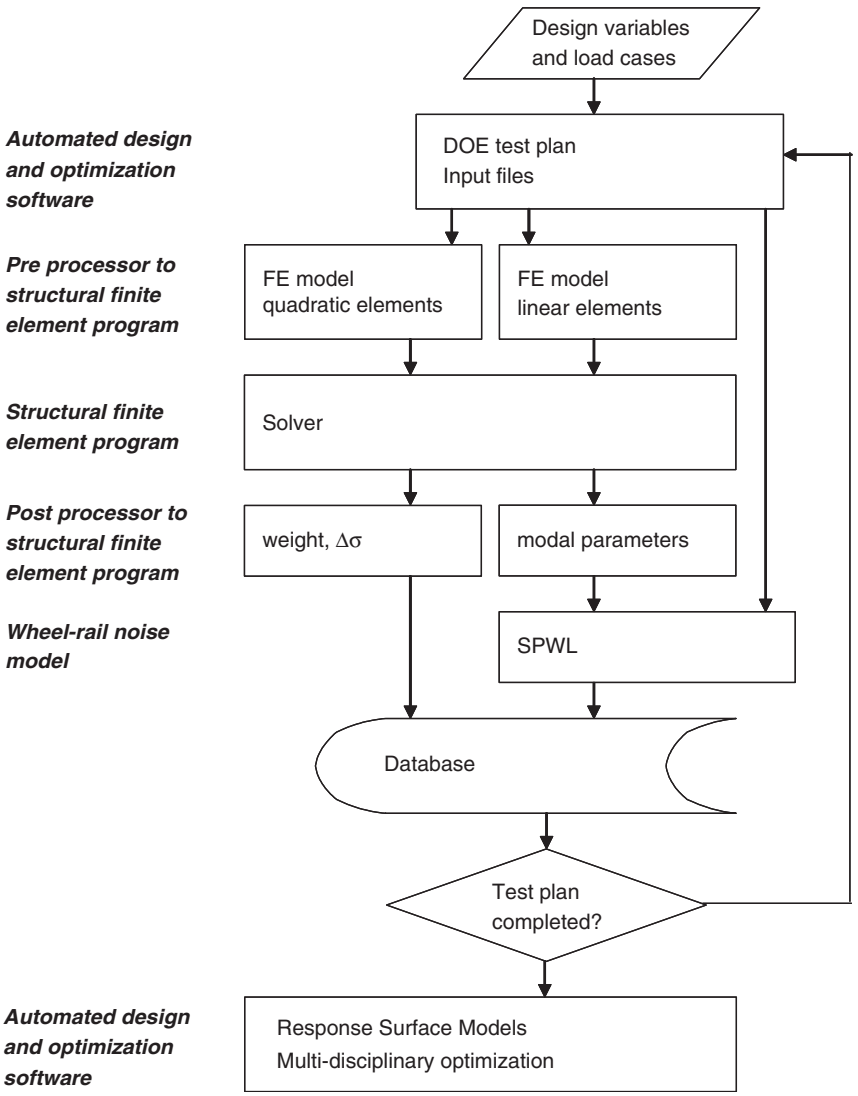

Fig. 1. Flow diagram illustrating the numerical procedure for multi-disciplinary optimization of railway wheels.

such as MSC/PATRAN, MSC/NASTRAN, MATLAB and TWINS [7] are combined for calculations of weight, modal parameters, bending stresses in the web and rolling noise. LMS OPTIMUS is adopted to drive and monitor the other computer programs, to visualize and explore the design space, and to identify the optimum design. The suggested approach is an automated design method in the sense that most of the analysis (such as generation of finite element (FE) models and editing of input files) is performed by the computer(s) without necessary involvement from the engineer(s).

2. Parametric FE model

A parametric FE model of a wheel has been developed that allows for computationally efficient investigations of different designs. The reference wheel design is based on the disc-braked Lucchini ETR470 monobloc wheel, which has a rather straight web and a lateral hub/rim offset of 15 mm. In the present application, the offset is the lateral distance between the nominal rolling circle (70 mm from the inside of the wheel rim) and a point 105 mm from the inside of the hub. In the reference design, the selected reference point on the hub is positioned 15 mm inside the nominal rolling circle. The web thickness varies between 15 and 26 mm depending on distance from the wheel centre.

In the present parametric model, four geometric design variables are used, as the scope is to demonstrate a design procedure rather than to exploit fully its possibilities. More variables (geometry, material, etc.) can be added if necessary. The selected design variables are wheel radius x_1, relative web thickness x_2, lateral offset x_3 between hub and rim, and the transition radii (fillets) x_4 between rim/web and web/hub, see Fig. 2. The design variable x_3 is measured from the position of the reference wheel offset. A positive value for x_3 means that the hub is moved outwards on the wheel axle (while the lateral rim position is maintained). Thus, when $x_3 = 15$ mm, there is no lateral offset between rim and hub. The boundaries of each variable when used in the demonstration below, and corresponding values for the reference wheel design, are listed in Table 1. The radial cross-sections of hub and rim are not altered between the different designs.

In each generation of a new FE model, the radial cross-sections of rim and hub are first positioned according to the given values on wheel radius and lateral offset (x_1 and x_3). The web shape is defined by using a third-order spline function that connects rim and hub. A modified web thickness is obtained by uniformly multiplying the reference (radius-dependent) web thickness with the factor $(1+x_2)$. The transition radii between rim/web and web/hub are generated by "fillet operations" in the FEM software. At the inside and

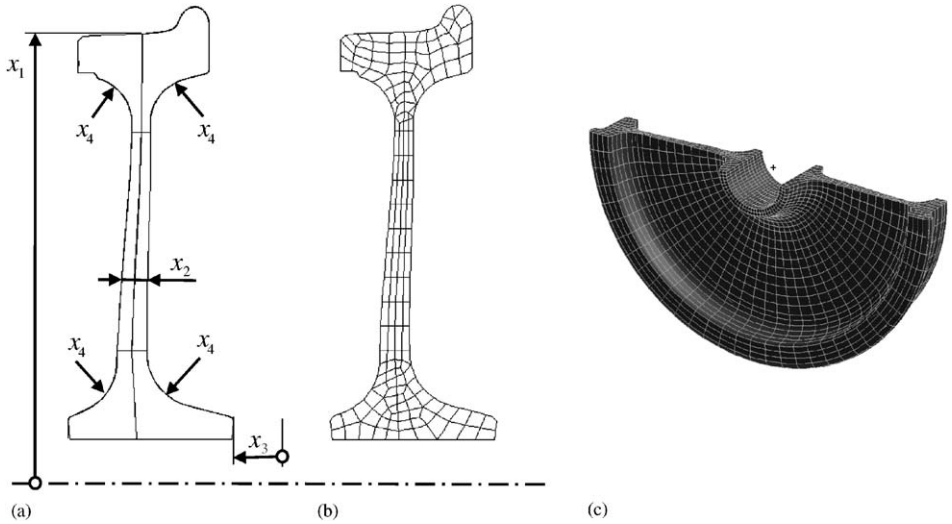

Fig. 2. (a) Geometric design variables x_i $(i = 1, 2, 3, 4)$ in the demonstration example, (b) two-dimensional mesh on the radial cross-section of the wheel, and (c) solid FE model of half a wheel for calculation of fatigue stress.

Table 1
Geometric design variables used in the optimization

Design variable	Description	Lucchini ETR470	Low boundary	High boundary
x_1	Wheel radius (m)	0.445	0.40	0.50
x_2	Web thickness (fraction)	0.0	−0.10	0.10
x_3	Lateral offset rim–hub (m)	0.0	−0.025	0.025
x_4	Transition radius (fraction)	0.93	0.70	0.93

outside transitions between rim and web, the maximum radius that can be generated between the tangents of the rim and web cross-sections is calculated. The minimum $R_{\min}$ of these two maximum radii is implemented. The curve radii between rim and web on the inside and outside of the wheel are assumed to be the same and equal to $R_{\min}$ multiplied by the variable x_4. The same procedure is adopted to define the radii at the two transitions between web and hub. A two-dimensional mesh is then generated on the completed radial cross-section of the wheel. The elements are swept into a three-dimensional solid FE mesh that corresponds to half a wheel. For calculation of mode shapes, a coarse mesh of linear hexahedral elements is used, whereas fatigue stresses are simulated using a more densely meshed FE model with quadratic hexahedral elements, see Fig. 1. Iterative mesh quality checks and element corrections are implemented in the procedure to generate models that are computationally accurate. Symmetry boundary conditions are used on the radial cross-section. Such an FE model allows for calculation of all wheel mode shapes except the circumferential ones, which can be neglected due to their lower radiation of noise. The inner surface of the hub is fixed. This means that the influence of the wheel axle on radiated noise is neglected. This is justified because wheel modes that are influenced by the wheelset axle bending and tension stiffnesses generally have higher damping than other modes, and they occur at relatively low frequencies where the track component of noise is dominating [7].

2.1. Numerical validation of the FE model

The parametric FE model that is based on the somewhat simplified geometry description explained above has been compared to an FE model that was generated directly from the ETR470 reference design. Eigenfrequencies of the two models deviate by $\pm 5\%$ in the frequency interval up to 6 kHz. The Modal Assurance Criterion (MAC) values show that there are significant differences between the calculated mode shapes (on-diagonal MAC values in the interval 0.4–0.99). However, comparisons of frequency response functions at the wheel–rail contact point show very good agreement. Note that perfect agreement between the parametric and reference design models was never a target, since it is the design procedure that matters.

3. High-cycle fatigue design

High-cycle fatigue properties of each generated wheel design are evaluated according to the draft standard prEN 13979-1 [8]. The objective is to ensure that wheel–rail contact loads will not induce fatigue cracking in the web. For each design, principal stresses are calculated at all FE nodes on the radial cross-section of the wheel (see Fig. 2) for three different load cases involving vertical and lateral contact loads corresponding to (1) a tangent track, (2) a circular curve and (3) negotiation of switches and crossings. The load cases are static, accounting for dynamic magnification factors according to the standard.

At a given FE node, the maximum principal stress $\sigma_{\max}$ and the corresponding critical load case (1, 2 or 3) are first identified. Then, the minimum principal stress $\sigma_{\min}$ (in the same direction as $\sigma_{\max}$) in the two remaining load cases is determined. The procedure is repeated for all nodes on the cross-section. The wheel meets the requirements for high-cycle fatigue design if $\Delta\sigma = \sigma_{\max} - \sigma_{\min} < 360$ MPa for all the nodes on the radial cross-section.

Table 2
Track input data used in TWINS

Track component	Property	
Rail	UIC60	
	Loss factor 0.02 (vertical and lateral)	0.02
	Cross receptance factor	–11 dB
Pad	Vertical stiffness	200 MN/m
	Lateral stiffness	40 MN/m
	Loss factor (vertical and lateral)	0.16
Sleeper	Rigid sleeper	
	Mass	400 kg
	Sleeper spacing	0.60 m
Ballast	Vertical stiffness	35 MN/m
	Lateral stiffness	12 MN/m
	Loss factor (vertical and lateral)	1.0

4. Rolling noise

The wheel component of rolling noise was calculated using the software TWINS (Track–Wheel Interaction Noise Software) [7]. Modal parameters (eigenfrequencies, mode shapes, modal masses and modal damping ratios) describe the dynamic properties of the wheel. Two identifiers are used to classify the different mode shapes: (i) the number of nodal diameters n ($n = 0, 1, 2, \ldots$) and (ii) the type of cross-sectional deformation being either an axial mode with m ($m = 0, 1, 2, \ldots$) nodal circles or a radial mode. For each wheel design, the automated work flow procedure in LMS OPTIMUS (automated design and optimization software in Fig. 1) edits most TWINS input files to describe the wheel geometry data, the set of modal parameters and to enforce the case naming convention used in the work flow. The lowest 45 modes were calculated and included in the analysis, spanning frequencies up to about 6 kHz. Modal damping ratios were based on recommendations in Ref. [7] that apply for a conventional undamped wheelset.

The track with UIC60 rails was modelled as a continuously supported Rayleigh–Timoshenko beam with rigid sleepers. Track input data correspond to an Italian high-speed line, see Table 2. The train speed and static wheel load are 220 km/h and 65 kN, respectively. A wheel–rail roughness spectrum typical for a disc-braked wheel on a good-quality track was used [9]. Wheel–rail contact was assumed to occur on the nominal rolling circle of the wheel with no lateral offset on the rail head.

5. Constrained layer damping

CLD on the web is also considered in the design to reduce vibrations and rolling noise. The visco-elastic material (with three alternative levels of thickness: 0.5, 1.0 or 1.5 mm) and the constraining steel layer (1 mm) are added on both sides of the web in the parametric FE model. The CLD covers the entire web from the outer radius of the hub to the inner radius of the rim. Shear modulus and damping loss factor of visco-elastic materials are dependent on frequency and temperature. Further, according to a manufacturer of such materials, the shear modulus can differ by a factor of 10 from one produced batch to another.

The influence of the CLD on eigenfrequencies was computed as a function of Young's modulus. The damping material frequency and temperature dependency could thereafter be translated into estimated modal damping and eigenfrequency as a function of temperature. However, the influence of the CLD on mode shapes and modal masses was neglected as the CLD is expected to show only minor influence on these.

In a verification step, two procedures for calculation of loss factors in the structural FE program were compared: the direct complex eigenvalue solution and the Modal Strain Energy (MSE) method. To simplify the comparison, a fictitious damping material without temperature or frequency dependence was used. The direct complex eigenvalue solution required approximately 149 min per wheel design, while the MSE

simulation was executed within 2 min. A comparison of the two methods showed that the MSE method, on average, underestimated wheelset damping by 8.3%. In comparison with the uncertainty in material data stated by the manufacturer and the influence of temperature on damping, this difference was regarded as negligible. Therefore, the loss factors η_1 that were used in the wheel–rail noise model were calculated according to

$$\eta_1 = \eta_0 + \eta_{\text{visc}} W_{\text{visc}}, \tag{1}$$

where η_0 is the loss factor for a conventional wheelset without any damping treatment (dependent on type of mode shape [7]), η_{visc} is the loss factor of the damping material, and W_{visc} denotes the fraction of the total strain energy (MSE method) that is associated with the damping layer when the wheel is vibrating with a given mode shape.

CLD on freight car wheels for a train speed 100 km/h was studied in Refs. [2,3]. The sound power level was reduced by around 5 dB in the 2 kHz and higher frequency bands, but not very much at lower frequencies. Since the contributions from the 2 kHz and higher frequency bands are more important in the overall sound power level at train speeds higher than 100 km/h, it was concluded that the reduction in overall level with the same damping treatment would be higher. In this case, the replacement of a tread-braked 920 mm standard freight wheel with a 860 mm wheel with an acoustically optimized cross-section and damping treatment led to a predicted reduction in A-weighted sound power of 7.9 dB.

6. Design of experiments and response surface models

As stated above, the target of the present study is to demonstrate a numerical procedure that can be used to design a wheel that meets the requirements for fatigue strength while minimizing the unsprung mass and rolling noise. This calls for a multi-disciplinary optimization approach that includes several types of analyses and software. The procedure is based on Design of Experiments (DOE) methodology and Response Surface Models (RSM) [10,11].

A fundamental step in the design process is to estimate the influence of variations in the design variables on critical responses. Estimated effects can be used to formulate empirical functions or RSM that approximate the responses in a limited region of the design space. Then an optimum set (in this region) of design variable levels can be found. A factorial design method serves the purpose of providing estimates of the effects that are caused by numerical variations in wheel design variables. In addition, the factorial design can detect and estimate interactions between parameters, i.e. cases where the effect of one design variable is strongly dependent on the numerical levels of other variables. This is an important advantage of a factorial design as compared to the more primitive method of varying one parameter at a time while keeping the other parameters constant.

A 3-level full factorial (3LFF) DOE was used to collect data points required to set up an approximate mathematical model relating design and response variables. This means that each design variable was assigned three levels (high, low and intermediate levels), and that all possible combinations of the design variables were investigated. Note that the need for high computational efficiency is of utmost importance when six or seven variables are used, while requirements are moderate when four design variables are considered, as the use of the 3LFF method and k variables implies execution of 3^k cases. The 3LFF with four design variables thus required simulations of $3^4 = 81$ wheel designs. The low and high levels are listed in Table 1. The intermediate levels were obtained by taking the arithmetic mean of the low and high levels.

The 3^k design allows for the modelling of a quadratic or higher-order relationship between response and design variables, depending on the number of executed cases and whether certain variable combinations can be discarded. A response y can then be represented by, e.g. a second-order model of the type

$$y = \beta_0 + \sum_{i=1}^{k} \beta_i x_i + \sum_{i=1}^{k} \beta_{ii} x_i^2 + \sum_{i} \sum_{\substack{j \\ i<j}} \beta_{ij} x_i x_j. \tag{2}$$

Eq. (2) represents a response surface in the k-dimensional design space with variables x_i. Estimated linear and quadratic effects and interactions between different design variables are denoted β_i, β_{ii} and β_{ij},

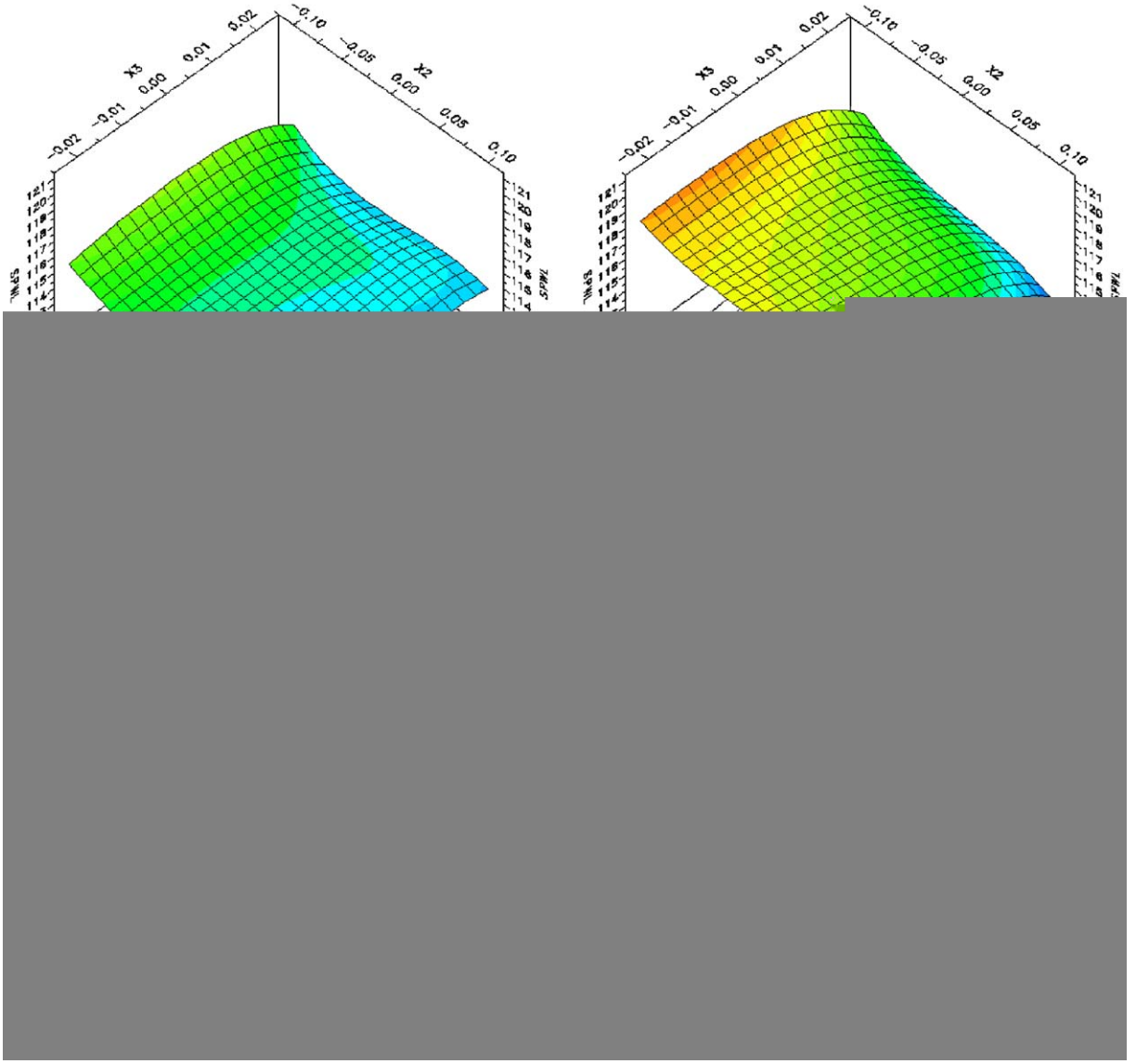

Fig. 3. Response surface models illustrating either A-weighted wheel sound power level SPWL [dB (re 1 pW)] or maximum fatigue stress range $\Delta\sigma$ (Pa) as a function of fractional change x_2 of the reference web thickness and lateral rim/hub offset x_3 relative to the reference wheel offset. (a) SPWL for wheel radius = 0.4 m, (b) SPWL for wheel radius = 0.445 m, (c) SPWL for wheel radius = 0.5 m, (d) $\Delta\sigma$ for wheel radius = 0.445 m.

respectively. If the fitted surface is an adequate approximation of the true response $\hat{y}$, then analysis of this surface will be approximately equivalent to analysis of the actual system. As an alternative, data can be fitted using a so-called kringing procedure in which the RSM explicitly fit computed data. Regression values are used to suggest whether to rely on the model of the kth order or the kringing RSM. The fit between RSM estimated and computed values is given by the ordinary regression value. The RSM "predictability" is estimated through a procedure in which an RSM is estimated for all data points except one. The difference between the computed and RSM estimated data points is computed and the procedure is repeated for all ensuing data points. A perfect RSM will have regression values of unity. Preference of whether to use an RSM of order k or the RSM obtained by the kringing procedure varies from one variable to another.

Data from the 81 cases were used to set up fourth-order polynomial RSM that establish the relations between weight, wheel sound power level (SPWL), fatigue stress and wheel geometry. The residual between the

RSM and computed values of the 81 cases showed that the SPWL is predicted by ± 0.5 dB (re 1 pW) or better and the regression values are 0.9946/0.9558 (fit/'predictability'). The wheel mass and the fatigue stress are predicted with an accuracy of ± 0.0007 kg (1.0/0.9995) and ± 12 MPa (0.9995/0.9969), respectively.

Examples of response surfaces from the demonstration example are illustrated in Fig. 3. The SPWL is dominated by three design variables: radius (x_1), web thickness (x_2) and lateral rim/hub offset (x_3). For the investigated range of the design variable settings, the SPWL can be modified by ± 4 dB. In summary, the SPWL is reduced by reducing the wheel radius, by increasing the lateral offset (straightening of the web), and by increasing the web thickness.

One example of a response surface illustrating fatigue stress, evaluated in accordance with the draft standard [8], as a function of web thickness and lateral offset is shown in Fig. 3(d). It is observed that many wheel designs lead to a $\Delta\sigma$ higher than the permitted level of 360 MPa. Increasing wheel radius and lateral offset between rim and hub increases the stress range $\Delta\sigma$. On the other hand, $\Delta\sigma$ is reduced by increasing web thickness and (to a smaller extent) transition radii between rim, hub and web. The influence of lateral hub/rim offset on rolling noise and fatigue stress illustrates one conflict that must be considered by the wheel designer. This clearly shows that wheel design is multi-disciplinary, as design of a low-weight wheel with acceptable fatigue properties would probably yield a noisy wheel, and vice versa that a low-weight and low-noise wheel may not withstand high-cycle fatigue.

7. Multi-disciplinary optimization

Self-adaptive genetic optimization algorithms were applied on the RSM to identify the wheel design that best fits the defined target. Optimization on the RSM is computationally efficient since each iteration does not require calculation of responses using the FE and wheel–rail noise models.

7.1. Wheel without CLD

The reference case defined in Table 1 and in Sections 3 and 4 leads to A-weighted SPWL of 116.7 dB (re 1 pW), wheel mass of 260.6 kg and stress range $\Delta\sigma$ of 306 MPa. This is the design that is the most similar to the ETR470 reference design, and all results calculated by the optimization procedure will be discussed with reference to this wheel. Table 3 illustrates the results from an optimization on the RSM when constraints are applied on wheel radius ($=0.445$ m), weight (<270 kg) and stress range (<355 MPa). As mentioned above, the anticipated accuracy of the RSM for SPWL is ± 0.5 dB (re 1 pW). It appears possible to design a wheel with SPWL of 113.0 dB (re 1 pW) and acceptable fatigue strength, if web thickness is uniformly increased by 8.8%, lateral hub/rim offset is increased by 23 mm (i.e. towards a more straight web design) and the radii between rim, web and hub are reduced. The wheel weight is increased by 9 kg. Note that the optimized design will be dependent on the selected constraints and load cases. Note also that the ETR470 reference wheel was designed for an existing wheel axle, thus constraining the lateral offset variable. The results of the current examination therefore do not reflect on the reference wheel design potential—it is merely used as a reference point for the optimization example.

Table 3
Comparison between reference and optimized (no CLD) wheel designs. Constraints are applied on wheel radius ($=0.445$ m), wheel weight (<270 kg) and stress range $\Delta\sigma$ (<355 MPa)

	Reference design	Optimized design
Wheel radius (m)	0.445	0.445
Web thickness (fraction)	0.0	0.088
Lateral offset rim–hub (m)	0.0	0.023
Radius (fraction)	0.93	0.74
SPWL [dB (re 1 pW)]	116.7	113.0
Weight (kg)	260.6	269.6
$\Delta\sigma$ (MPa)	306	347

7.2. Wheel with CLD

A new 3LFF DOE was performed to collect data points required to set up RSM for a wheel with CLD. The wheel radius was set to 0.445 m. The best performance of the CLD was obtained when the thickness of the visco-elastic material was set to 0.5 mm. Examples of response surfaces illustrating SPWL as a function of lateral hub/rim offset and web thickness, without and with CLD, are shown in Fig. 4. Visco-elastic material with maximum or minimum damping performance depending on production batch was considered. It was found that the combination of CLD and shape optimization was effective in reducing the radiated wheel SPWL. However, the performance of the visco-elastic material varies so much between production batches that its effect on reducing the SPWL varies from 0 to 6 dB. For this application, performance is guaranteed only from selected batches of the damping material, or a change of damping material to one with a more narrow tolerance. A combination of wheel shape and CLD optimization, considering fatigue stress requirements, indicates that the SPWL can be reduced by 11 dB to 105.6 dB (re 1 pW) at 20 °C if a mass increase of 14 kg to 280 kg can be accepted. The constraining layer and the shape optimization each account for about half of the mass increase. For the investigated load case with the applied constraints on wheel radius and maximum fatigue stress, the optimum wheel shape is shown in Fig. 5. The position of the hub is moved 25 mm outwards on the axle relative to the rim ($x_3 = 25$ mm). The web thickness is increased and the radii between web and rim/hub are decreased. Note that, since the value of the design variable x_3 is at the boundary of the explored design space, the derived design is not a true optimum in this case.

7.3. SPWL versus weight for an optimized wheel

In an additional exercise, the RSM have been used to determine the minimum wheel mass accounting for the constraint that SPWL must not exceed a certain level. To produce Fig. 6, the optimization procedure was repeated for various settings of the SPWL constraint. Requirements on fatigue strength, and wheels with or without CLD, were considered. The reference case is indicated at 116.7 dB (re 1 pW) and zero mass change. The CLD with a 1 mm thick constraining steel layer adds about 7 kg to the wheel mass in Fig. 6, which is why the damping material with poor performance only adds weight. It is observed that shape optimization and CLD with maximum damping performance can be combined to design a wheel with a 3 dB reduction in SPWL and a simultaneous reduction in wheel mass by around 9 kg relative to the reference case, see (1) in Fig. 6.

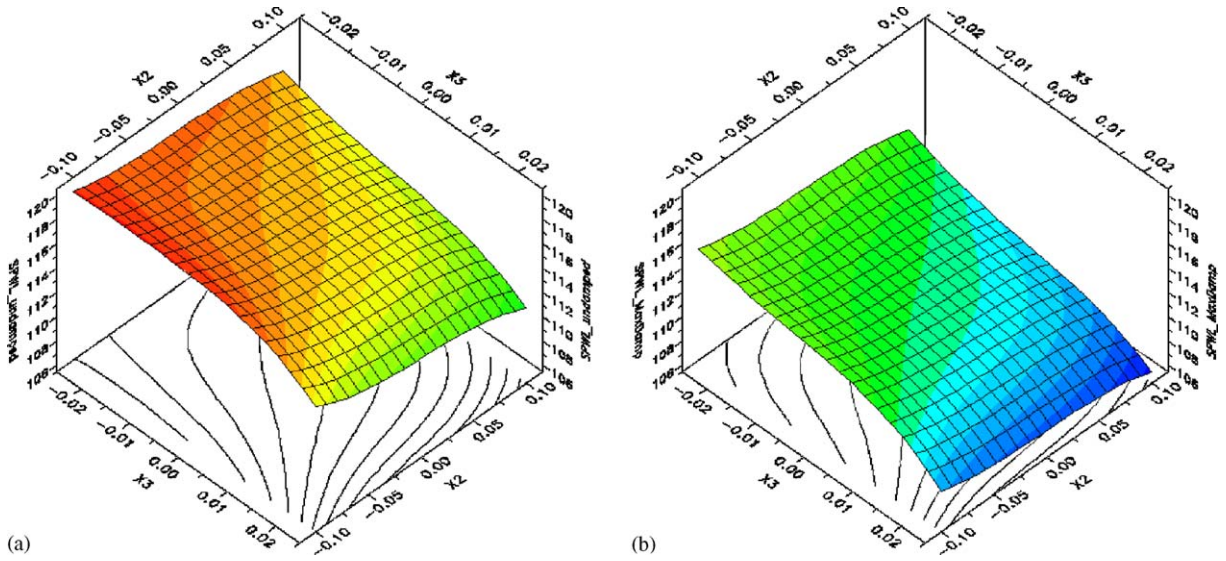

Fig. 4. Response surface models illustrating A-weighted wheel sound power level (SPWL) [dB (re 1 pW)] as a function of fractional change x_2 of the reference web thickness and lateral rim/hub offset x_3 relative to the reference wheel offset. Wheel radius = 0.445 m. (a) No CLD, (b) CLD with maximum damping performance of the visco-elastic material and thickness 0.5 mm.

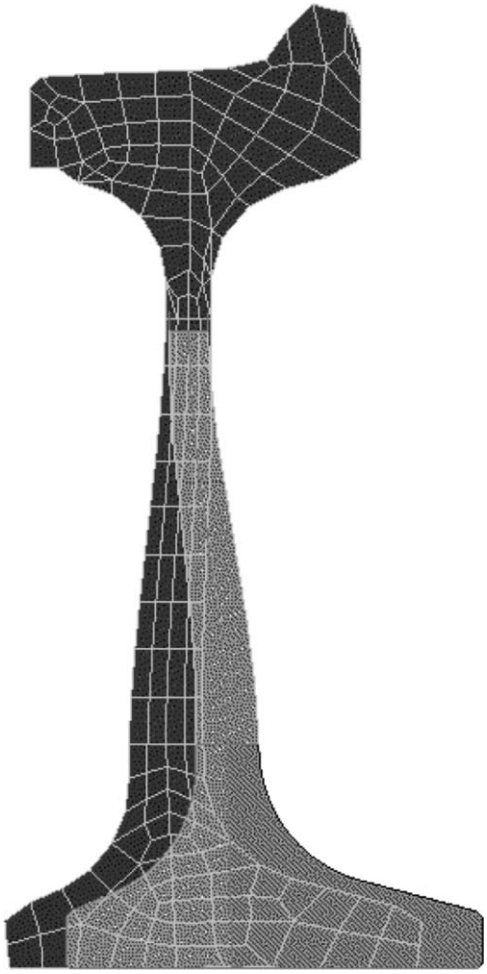

Fig. 5. Reference (grey) and shape optimized (black) wheel geometry.

Further, the CLD is only effective when the selected damping material is of high quality, see the dashed curve (2) illustrating the case with maximum damping. For a given wheel mass, damping the wheel brings a maximum reduction in SPWL of 4–6 dB, see (3). The maximum SPWL reduction of around 11 dB is achieved through a simultaneous increase in wheel mass of about 14 kg and use of damping, see (4).

8. Discussion on how to extend and further exploit the approach

The four design variables selected for the work of this paper were suggested to the authors by the HIPERWHEEL project partners and were based on many years of product experience. However, investigating a product where such a priori knowledge is not available, the approach would be first to define a much larger set of design variables, issue a screening DOE test plan, e.g. a Taguchi test plan [10], to identify the dominant and second-order design variables. A sampling DOE is thereafter issued for the dominant design variables, using e.g. the 3LFF method, and RSM are set up.

The optimum wheel design, as identified by the RSM, is an approximation and it should be verified by a computation (again using the automated workflow) where the variables are set to the values of the RSM-based optimum. A fine-tuning design loop can be conducted by performing a new iteration with the numerical procedure based on smaller ranges in design variables in the vicinity of the first RSM optimum.

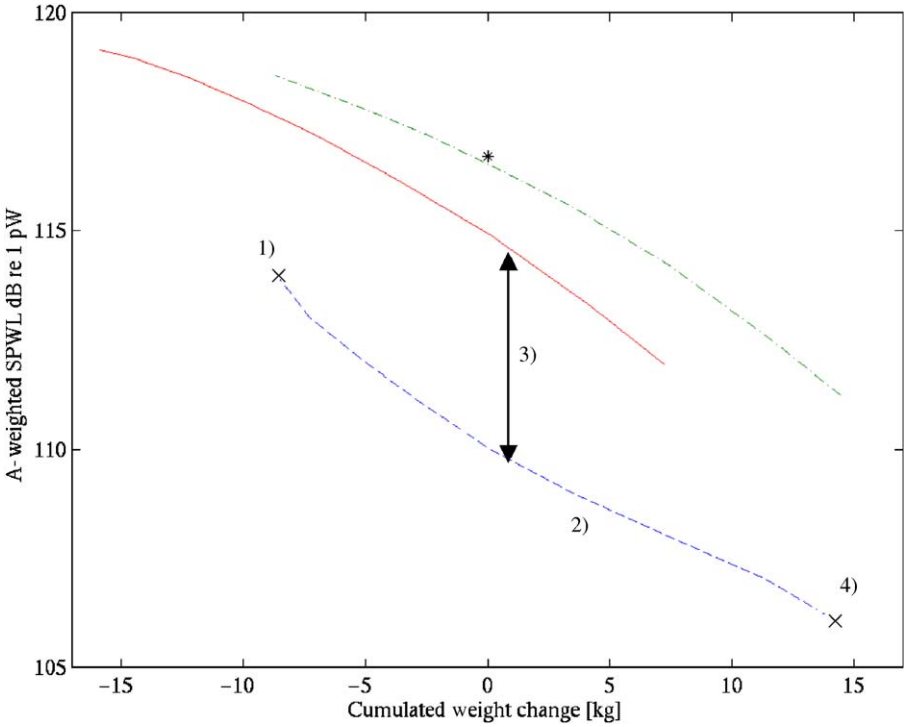

Fig. 6. Example illustrating wheel sound power level versus weight for a wheel with shape optimization and CLD. Wheel radius = 0.445 m and thickness of visco-elastic material = 0.5 mm. Solid line: no CLD; dashed line: maximum CLD performance; dash–dotted line: minimum CLD performance; asterisk: reference design.

The automated workflow can then be driven by, e.g. a gradient-based optimizer, or a DOE can be set up for a narrower data range.

An important aspect of automating the work flow is the ability for knowledge dissemination within the project team. Parts of the work flow can be built up by different experts and thereafter executed by non-experts, or analysis can be divided and distributed for analysis at multiple sites containing software/expertise needed for the job.

9. Concluding remarks

DOE methodology and automated design have been combined to develop a computationally efficient numerical procedure for multi-disciplinary optimization of railway wheels. In a demonstration example, rolling noise, unsprung mass and fatigue stress have been considered using wheel radius, web thickness, lateral hub/rim offset and CLD as design variables. In the example where wheel shape optimization without damping was studied (Section 7.1), the 81 wheel designs were executed and analysed in 2.5 h on a HP C3600 computer (structural FE program) and a Pentium II PC with 128 MB RAM (wheel–rail noise model).

The approach is open for concurrent engineering at multiple sites when the work flow is used to generate models and input data that are executed elsewhere and output data are collected into the work flow in a final post-processing stage. This concurrent engineering feature was exploited for the acoustic analyses that were made "offline" on an unnetworked computer and data were transferred through electronic mail between the operators.

To increase the robustness of the optimized wheel design, the number of investigated load cases affecting rolling noise needs to be increased. Several train speeds, contact positions at different lateral offsets from the nominal running position of the tread, different shapes of wheel–rail roughness spectra, and different temperatures affecting the performance of the visco-elastic material should be addressed. This can be handled

efficiently by the proposed procedure. Constraints on the wheel design need to be specified by the wheel manufacturer. Using information about the wheel geometry, it is anticipated that other factors such as the cost for manufacturing of the wheel can be added in the multi-disciplinary approach.

Acknowledgements

The work reported in this paper was carried out as part of the European Community funded project HIPERWHEEL (contract number: G3RD-CT-2000-00244) where the main objective was to develop an "Innovative High Performance Railway Wheelset". Input data for the reference design were supplied by Mr. Steven Cervello of Lucchini CRS. The partners in CHARMEC are Abetong Teknik, Banverket, Bombardier Transportation Sweden, Duroc, Green Cargo, Interfleet Technology AB, Lucchini Sweden, SAB WABCO, SL Infrateknik and voestalpine Bahnsysteme. Financial support is also provided by the governmental agency VINNOVA.

References

[1] M. Fermér, Optimization of a railway freight car wheel by use of a fractional factorial design method, *Proceedings of the Institution of Mechanical Engineers Part F Journal of Rail and Rapid Transit* 208 (1994) 97–107.
[2] C.J.C. Jones, D.J. Thompson, A. Frid, M. Wallentin, Design of a railway wheel with acoustically improved cross-section and constrained layer damping, in: *Proceedings of Internoise*, Vol. 2, Nice, France, 2000, pp. 673–678.
[3] C.J.C. Jones, D.J. Thompson, Rolling noise generated by wheels with visco-elastic layers, *Journal of Sound and Vibration* 231 (2000) 779–790.
[4] S. Cervello, G. Donzella, A. Pola, M. Scepi, Analysis and design of a low-noise railway wheel, *Proceedings of the Institution of Mechanical Engineers Part F Journal of Rail and Rapid Transit* 215 (2001) 179–192.
[5] J.C.O. Nielsen, A. Igeland, Vertical dynamic interaction between train and track—influence of wheel and track imperfections, *Journal of Sound and Vibration* 187 (1995) 825–839.
[6] A. Daneryd, J.C.O. Nielsen, E. Lundberg, A. Frid, On vibroacoustic and mechanical properties of a perforated railway wheel. in: *Proceedings of the sixth International Workshop on Railway Noise*, Ile des Embiez, France, 1998, pp. 305–317.
[7] M.H.A. Janssens, D.J. Thompson, F.G. de Beer, TWINS version 3.0 User's Manual, TNO report HAG-RPT-000020, TNO Institute of Applied Physics, Delft, The Netherlands, 2000.
[8] European Committee for Standardization (CEN), Draft prEN 13979-1, Railway applications—wheelsets and bogies—wheels, Technical approval procedure, part 1: forged and rolled wheels, September 2000.
[9] D.J. Thompson, Definition of the reference roughness, Institute of Sound and Vibration Research, University of Southampton Technical Document 3S7J28T1.DA, 1997, 10pp.
[10] G.E.P. Box, W.G. Hunter, J.S. Hunter, *Statistics for Experimenters*, Wiley, New York, 1978.
[11] D.C. Montgomery, *Design and Analysis of Experiments*, Wiley, New York, 1984.